Journal of Alloys and Compounds 505 (2010) 793–800

Contents lists available at ScienceDirect

Journal of Alloys and Compounds

journal homepage: www.elsevier.com/locate/jallcom

Elastic properties and thermal behavior of Sn–Zn based lead-free solder alloys

A.A. El-Daly*, A.E. Hammad

Physics Department, Faculty of Science, Zagazig University, Zagazig, Egypt

ARTICLE INFO

Article history:
Received 1 May 2010
Received in revised form 17 June 2010
Accepted 22 June 2010
Available online 1 July 2010

PACS:
62.20.Fe
61.82.Bg
61.66.Dk

Keywords:
Lead-free solder
Sn–Zn alloy
Microstructure
Ultrasonic velocity
Thermal properties
Elastic properties

ABSTRACT

In this study, the effects of separate and dual additions of small amount of Cu, In and Ag on the microstructure and elastic properties as well as thermal behavior of the eutectic Sn–9Zn solder alloy were investigated. The elastic properties of the newly developed ternary and quaternary alloys have been investigated using sound wave velocity measurements at 4 MHz and $T = 25\,^{\circ}C$. In particular, the hardness, the attenuation coefficient, the bulk and shear moduli, Young's and Poisson's ratio have been established for a range of alloy compositions. Results showed that alloying of Cu, In and Ag resulted in reducing fusion heat, solidus temperature and broadening the pasty range. Moreover, the presence of additional elements in Sn–Zn alloy system allows many complex intermetallic (IMC) phases to form. Both the hardness and reduced modulus increase as the Poisson's ratio of the alloy decreases. The elastic properties can be correlated with the formation of the new IMC phases. By analyzing the quotient of shear modulus to bulk modulus, we can assume that the Sn–9Zn, Sn–9Zn–1.5Ag and Sn–9Zn–0.7Cu alloys are ductile solders whereas, the Sn–9Zn–1.5In and Sn–9Zn–1.5Ag–0.7Cu alloys are brittle in nature.

1. Introduction

Increased health concerns over the toxicity of Pb in eutectic Sn–Pb solders have promoted the development of new lead-free solder alloys for electronic packaging [1]. Among the various lead-free solders, eutectic Sn–Zn solder alloy has so far received much attention and emerged as possible replacements for Sn–Pb solders because of its low melting point, excellent mechanical properties and low cost. However, its main disadvantage of poor oxidation resistance and wetting properties caused by the high activity and corrosion susceptibility of Zn prevents its wide practical applications, especially in the critical part of electronic packaging products. Studies on the improvement of their overall wetting and mechanical properties have been widely investigated and progress has been made by adding different alloying elements, such as Ag, Cu, Bi, In, Ge and ZrO_2 nanoparticles [2–7].

Previous studies showed that the proper addition of Cu in Sn–Zn solders is effective way to avoid the formation of Au–Zn IMCs between the interface with Sn–Zn and Au and improve the wetting properties [2,3]. Recently, Wang et al. [4] reported that the addition of Ge could effectively improve the anti-oxidation capability, electrical resistance, thermal expansion behavior and mechanical strength of $Sn_{84}Zn_{13}$ Bi_3 solder alloys. Our previous works [5,6] indicate that the addition of small amount of Bi could effectively improve the overall thermal and mechanical properties of the eutectic Sn–Zn solder alloy. On the other hand, the effects of separate and dual addition of small amount of Ag and Cu on the microstructure and mechanical properties of the eutectic Sn–9Zn solder alloy were also investigated. It was found that the proper additions of Ag and/or Cu in Sn–Zn solders are beneficial to encourage the formation of new Ag–Zn, Cu–Zn and Cu–Sn IMCs. These IMCs play an important role in mechanical properties of the Sn–9Zn solder alloy. For example, single addition of Ag led to formation of AgZn, Ag_5Zn_8 and ε-$AgZn_3$ IMCs, which results in significant increase in both ultimate tensile strength (UTS) and ductility, while, the flower shaped and rod shaped Cu_6Sn_5, γ-Cu_5Zn_8 and ε-$CuZn_5$ IMCs produced by Cu alloying, results in small increase in UTS and ductility. Moreover, the dual addition of Ag and Cu suppressed the appearance of Ag–Zn IMCs due to the competition for Zn between Cu and Ag, which results in slight decrease in UTS and ductility of Sn–9Zn–1.5Ag solder. Efforts are still needed to further improve the overall mechanical properties of this type of alloys and to discover the determining factors that control the reliability of the Sn–9Zn solder.

However, the elastic constants are one such material property that builds a foundation for a better understanding of various other properties such as mechanical, physical or even electronic. Lately, elastic constants have been correlated to properties like hardness,

* Corresponding author. Tel.: +20 552325030; fax: +20 552308213.
E-mail address: dreldaly99@yahoo.com (A.A. El-Daly).

0925-8388/$ – see front matter © 2010 Elsevier B.V. All rights reserved.
doi:10.1016/j.jallcom.2010.06.142

fracture toughness, stiffness, ductility and bond characteristics. Elastic constants are also vital in considering defects in solids such as vacancies, interstitials, substitutional impurities, dislocations, twin boundaries and grain boundary energies [8–11]. Moreover, they are associated with specific heat, thermal expansion and Debye temperature. Therefore, knowledge of such material property will be of great interest in understanding their behavior under different constraints [12]. Nevertheless, no studies have been concentrated on the effect of Ag and Cu on the elastic constants of eutectic Sn–Zn solder alloy using pulse echo technique. Pulse echo technique [13] is an important method for probing the elastic constants of materials. This is associated with the fact that the ultrasonic wave velocity is functionally related with elastic constants of the material which, in turn, depends on the chemical composition as well as the structure and stressed state of the material [14,15]. Moreover, ultrasonic waves are inexpensive, quick, sensitive, nondestructive method and easier physical interpretation of a principal constraint situation compared to the traditional tensile testing. This provides a highly desirable way to probe and image the interior of opaque objects.

The purpose of this work is to identify the effects of separate and dual addition of small amounts of Ag, In and Cu on the thermal behavior and elastic constants of the eutectic Sn–9Zn solder alloy. The key factors that affect the thermal and elastic behavior of the solder alloy are discussed. Hopefully, these small elements additions can play a positive role on the improvement of the overall thermal and elastic properties of the Sn–9Zn-based alloys. The results are wished useful in the further development of new solder alloys for different electronic packaging applications.

2. Experimental

2.1. Materials and experimental procedure

In the present work, the lead-free solder alloys with the compositions (wt.%) of Sn–9Zn eutectic, Sn–9Zn–0.7Cu, Sn–9Zn–1.5Ag, Sn–9Zn–1.5In and Sn–9Zn–1.5Ag–0.7Cu were prepared from Sn, Zn, Ag, In and Cu (purity 99.97) as raw materials. The process of melting was carried out in a vacuum arc furnace under a high purity argon atmosphere to produce rod-like specimen with a diameter of approximately 10 mm. The molten alloys were homogenized at 500 °C for 1 h and then poured in a steel mold to prepare the chill cast ingot. A cooling rate of 6–8 °C/s was achieved, so as to create the fine microstructure typically found in small solder joints in microelectronic packages [5]. Consequently, chemical analyses were done by volumetric method to determine the exact composition of the casting ingots. The chemical compositions of the five solder alloys are listed in Table 1. Differential scanning calorimetry (DSC) (Shimadzu DSC-50) was carried out to understand the melting process of the five solder alloys. Heating the specimens in DSC was carried out at 5 °C/min of heating rate in Ar flow. The evolution of microstructure for all solder alloys and phase identification of the alloy samples were carried out by X-ray diffractometry (XRD) at 40 kV and 20 mA using Cu Kα radiation with diffraction angle (2θ) from 25° to 85° and a constant scanning speed of 1°/min. The solder ingots were then mechanically machined into a wire samples with a gauge length marked 5×10^{-2} m for each samples and 1.5×10^{-3} m in diameter. Tensile tests were carried out with a tensile testing machine (Instron 3360 Universal Testing Machine). The tests were carried out at constant strain rate of $1.8 \times 10^{-3}\ s^{-1}$ and temperature of 25 °C. The curves represent average results of tensile tests carried out with three different specimens. The environment chamber temperature could be monitored by using a thermocouple contacting with specimen.

2.2. Ultrasonic velocity measurement

In order to measure the ultrasonic velocity, accurately, each alloy sample was first polished with 0.5 μm Al_2O_3 particles. The polished specimens are cylindrical in shape and have a length of 6 mm and a diameter of 10 mm in the gauge section. Plane parallelism between opposite faces was checked using a surface plate and its accuracy was ±25 μm. The ultrasonic velocities were obtained using pulse echo technique. The transit time between the initiation and the receipt of the pulse appearing on the screen of a flaw detector (USIP20-Kraütkramer) was measured using a standard electronic circuit (Hewlett Packard 54615 B). The ultrasonic wave velocity was therefore, calculated by dividing the round trip distance (twice the thickness of the sample) by the elapsed time according to the following relation:

$$V = \frac{2x}{\Delta t} \tag{1}$$

where x is the sample thickness and Δt is the time interval. All velocity measurements in this study were done at 4 MHz frequency, and at room temperature (25 °C). By using the Karl Deutsch transducer S12 HB4 with fundamental frequency of 4 MHz and the Kraütkramer transducer K4KY with fundamental frequency of 4 MHz, the longitudinal and shear ultrasonic wave velocities were estimated, respectively. Owing to the high accuracy of the setup, the ultrasonic wave velocity measurements with an error in the order of ±19 m/s for longitudinal velocity (V_l) and ±7 m/s for shear velocity (V_s) were determined.

2.3. Density measurement

The density (ρ) of each alloy samples was measured by applying Archimedes principle at 25 °C using toluene as an immersion liquid and applying the relationship:

$$\rho = \rho_b \frac{w_a}{w_a - w_b} \tag{2}$$

where ρ_b is the density of the buoyant. w_a and w_b are the sample weights in air and the buoyant, respectively. The experiment was repeated three times, and the estimated error in density measurement for all alloy samples is ±5 kg/m^3.

2.4. Determination of elastic moduli

For an isotropic solid, a number of researchers have given the empirical relationships to relate shear modulus (G), Young's modulus (E), bulk modulus (K) and Poisson's ratio (υ) for various elements. Poisson's ratio (υ) is reported to provide more information about the character of the bonding forces than any of the other elastic coefficients [16,17].

Poisson's ratio (υ) is related to E and G by (3):

$$\upsilon = \frac{E}{2G} - 1 \tag{3}$$

Poisson's ratio (υ) also is related to ultrasonic longitudinal wave velocity (V_l) and shear wave velocity (V_s) by (4):

$$\upsilon = \frac{V_l^2 - 2V_s^2}{2(V_l^2 - V_s^2)} \tag{4}$$

Additionally, V_l and V_s are related to E and G by (5):

$$E = \frac{3\rho V_s^2[V_l^2 - (3/4)V_s^2]}{(V_l^2 - V_s^2)} \tag{5}$$

$$G = \rho V_s^2 \tag{6}$$

where ρ is the density.

The differential relationships of υ with (E and G) and (V_l and V_s) can be obtained by differentiating Eqs. (3) and (4), respectively. The differential forms of the above equations are:

$$\frac{d\upsilon}{\upsilon} = \frac{1}{(1 - 2G/E)}\left(\frac{dE}{E} - \frac{dG}{G}\right) \tag{7}$$

$$\frac{d\upsilon}{\upsilon} = \frac{2V_l^2V_s^2}{(V_l^2 - V_s^2)(V_l^2 - V_s^2)}\left(\frac{dV_l}{V_l} - \frac{dV_s}{V_s}\right) \tag{8}$$

It can be seen from Eqs. (7) and (8) that the variation in Poisson's ratio depends upon the variations in E and G and their relative values Eq. (7). Similarly, the relative variations in V_l and V_s also affect the variation in Poisson's ratio Eq. (8). It is to be noted that in any material, E and G, as well as V_l and V_s, tend to vary in the same direction (increase or decrease). Hence, it is difficult to deduce from Eqs. (7) and (8)

Table 1
Chemical composition of the five solder alloys (wt.%).

Alloys	Zn	Ag	Cu	In	Pb	Bi	Sb	As	Sn
Sn–9Zn	8.97	–	–	–	0.012	0.007	0.011	0.006	Bal.
Sn–9Zn–1.5Ag	8.95	1.49	–	–	0.014	0.009	0.016	0.008	Bal.
Sn–9Zn–0.7Cu	8.96	–	0.72	–	0.014	0.010	0.019	0.009	Bal.
Sn–9Zn–1.5In	8.95	–	–	1.49	0.014	0.009	0.016	0.008	Bal.
Sn–9Zn–1.5Ag–0.7Cu	8.99	1.52	0.71	–	0.017	0.013	0.021	0.012	Bal.

Table 2
Comparison of solidus temperature (T_{onset}), liquidus temperature (T_{end}) and fusion heat (ΔH) for various solder alloys.

Solder alloys	T_{onset} (°C)	T_{end} (°C)	Pasty range (°C) ($T_{end} - T_{onset}$)	Melting temperature (°C) (peak)		ΔH (J/g)		Reference
				P_1	P_2	ΔH_{P_1}	ΔH_{P_2}	
Sn–37Pb	179.5	191.0	11.5	183.0	–	104.2	–	[17]
Sn–5Sb–3.5Ag	216.0	226.8	10.8	222.48	–	191.4	–	[17]
Sn–9Zn	197.9	201.9	4.0	199.1	–	157.9	–	This study
Sn–9Zn–1.5Ag	196.8	209.4	12.6	198.7	206.5	88.5	21.6	This study
Sn–9Zn–0.7Cu	191.5	202.4	10.9	196.8	199.2	29.9	81.2	This study
Sn–9Zn–1.5In	191.5	201.5	10.0	198.4	–	127.4	–	This study
Sn–9Zn–1.5Ag–0.7Cu	196.9	215.4	18.5	198.5	212.7	56.1	45.2	This study

whether the variation of υ would be in the same or opposite direction to that of the elastic constants, E and G. The nature of the variation of υ would therefore depend on whether G or E is affected more by metallurgical variables. For, if the rate of change of E (or V_l) is more than that of G (or V_s), then the right hand side of Eqs. (7) and (8) will be positive, and hence υ will vary in the same direction as that of E and G (or V_l and V_s). Similarly, if the rate of change of G (or V_s) is more than that of E (or V_l), the right hand side of Eqs. (7) and (8) will be negative, and hence υ will vary opposite to E and G (or V_l and V_s). From the first law of thermodynamics, it can be seen that E, K and G are positive, and since $K = E/3(1 - 2\upsilon)$ and $G = E/2(1 + \upsilon)$. However, for isotropic solids, υ is bounded practically by 0 and 1/2. For $\upsilon = 1/2$, no volume change occurs during deformation [17]. Attenuation coefficients α were calculated from the echo height ratio of the consecutive peaks according to the relationship

$$\alpha = 20\frac{\log(A_i/A_j)}{2x} \quad (9)$$

where A_i and A_j are the echo heights of consecutive peaks i and j, respectively, and d is the specimen thickness in mm.

3. Results and discussion

3.1. X-ray diffraction analysis

For determination of the phases that appeared in the five solder alloys, the as-solidified alloys were examined by XRD, as shown in Fig. 1(a)–(e). It can be seen that the β-Sn matrix and the precipitated α-Zn phase are the main constituents in the five as-cast alloys. However, the alloys containing Ag, In and Cu exhibited additional IMCs such as AgZn, γ-Ag_5Zn_8 and ε-$AgZn_3$ for Ag-containing solder, Cu_6Sn_5, γ-Cu_5Zn_8 and ε-$CuZn_5$ for Cu-containing solder, and In_3Sn for In-containing solder, along with the peaks of β-Sn phase and α-Zn phase in all alloys. It is also seen that the intensity of the eutectic α-Zn phase decreased in the Ag, In and Cu-containing alloys, as shown in Fig. 1. Hence, the formation of Ag–Zn, In–Sn or Cu–Zn compounds reduces the Zn content in the alloy matrix and enhances the formation of the hypoeutectic structure in both the ternary and quaternary solder alloys.

3.2. Thermal properties

To identify the fundamental thermal reactions of the solder alloys on heating, the as-cast Sn–9Zn eutectic, Sn–9Zn–1.5Ag, Sn–9Zn–0.7Cu, Sn–9Zn–1.5In and Sn–9Zn–1.5Ag–0.7Cu alloys were analyzed by DSC, as shown in Fig. 2. The DSC results are summarized in Table 2. With the addition of small amount of Ag, In and Cu elements, the eutectic temperature of Sn–9Zn changed only slightly. The eutectic temperatures were 198.7, 196.8, 198.4 and 198.5 °C for the Sn–9Zn–1.5Ag, Sn–9Zn–0.7Cu, Sn–9Zn–1.5In and Sn–9Zn–1.5Ag–0.7Cu, respectively, as compared with 199.1 °C for Sn–9Zn eutectic alloy. It is also found that the only endothermal peak for the Sn–9Zn samples was separated into double peaks for the Ag and Cu-containing samples. The first peak at low temperatures is the eutectic temperature of the Sn–Zn binary system, and the second peak at high temperatures corresponded to the melting temperature of the primary β-Sn phase and the liquidus line of the newly developed ternary and quaternary solder alloys. Similar results are obtained by Lee et al. [18]. However, the height of the first peak decreased with the addition of small amount of Ag and Cu elements. The Zn atoms in Sn–Zn alloy are captured by Ag and Cu additives, resulting in the formation of Ag–Zn and Cu–Zn IMCs, which leads to decrease the first peak and increase the melting range. XRD analyses were carried out to clarify the composition of the new phases. And interestingly it was found that these Zn form IMCs of two different types with both Ag and Cu separately, as can be seen in Fig. 1(b)–(d).

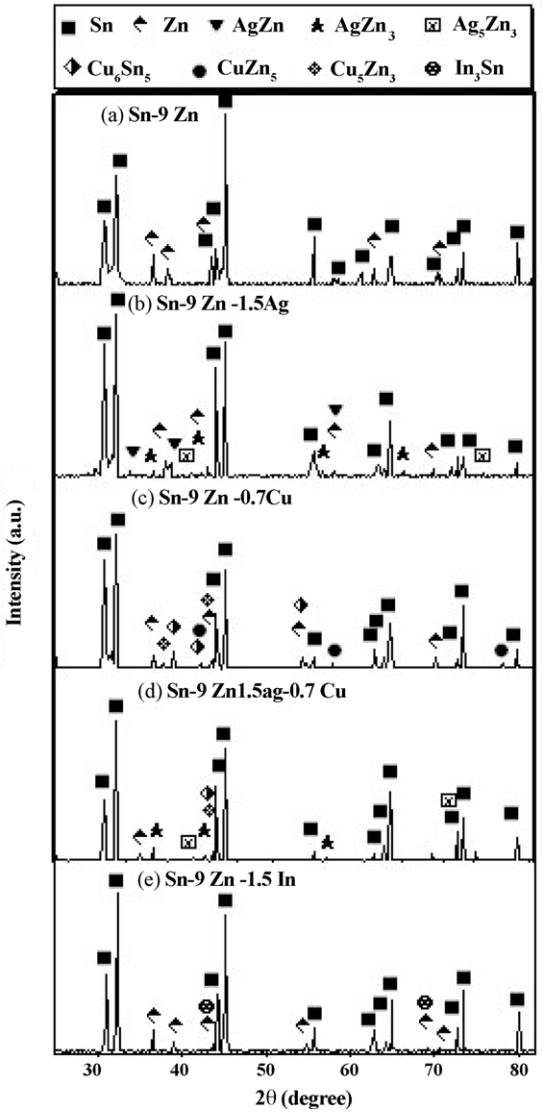

Fig. 1. XRD patterns of (a) Sn–9Zn, (b) Sn–9Zn–1.5Ag, (c) Sn–9Zn–0.7Cu, (d) Sn–9Zn–1.5Ag–0.7Cu and (e) Sn–9Zn–1.5In alloys.

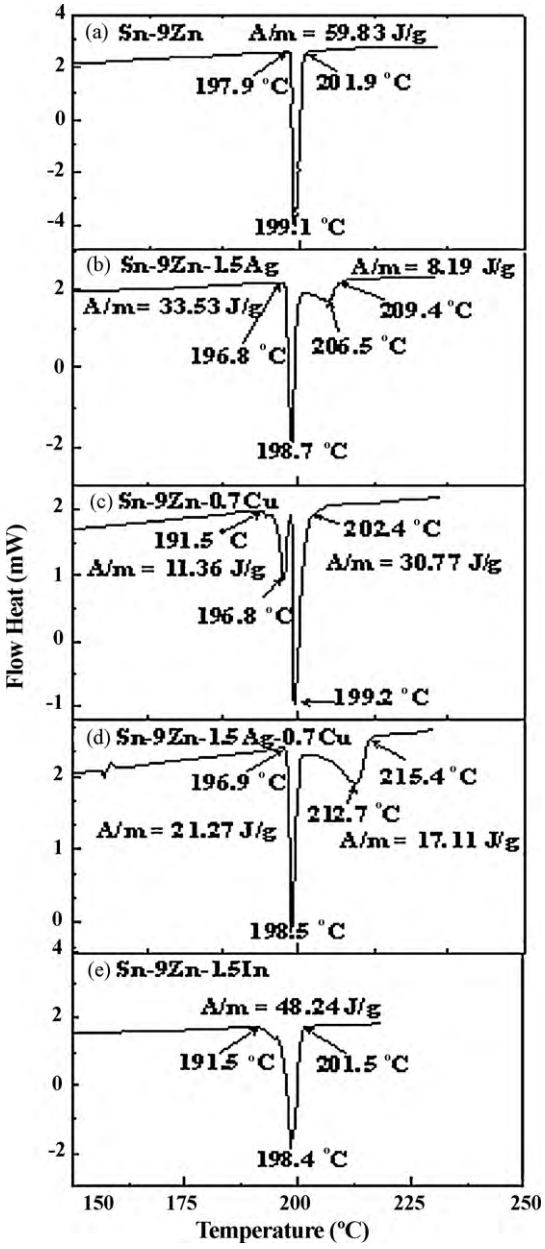

Fig. 2. DSC curves of (a) Sn–9Zn, (b) Sn–9Zn–1.5Ag, (c) Sn–9Zn–0.7Cu, (d) Sn–9Zn–1.5Ag–0.7Cu and (e) Sn–9Zn–1.5In solder alloys.

On the other hand, with the additions of In, Ag and/or Cu elements, the eutectic Sn–9Zn alloy exhibited additional change in the solidus (T_{onset}) and liquidus (T_{end}) temperatures. The T_{onset} decreased whereas, the T_{end} increased in the ternary and quaternary alloys (see Table 2). The pasty range value, which is the difference between the T_{end} and T_{onset} temperatures, is very important in electronic soldering and other industrial applications. Table 2 shows that the addition of small amount of Ag or Cu expands rather the pasty range ($T_{end} - T_{onset}$). 1.5% of In and Ag additions increase the measured pasty range of Sn–9% Zn from 4 to 10.0 and 12.6 °C, respectively, whereas, the addition of an amount of 0.7% Cu increases it to 10.9 °C only, which is lower than 11.5 °C for Sn–Pb eutectic [19]. In contrast, pasty range of Sn–9Zn–1.5Ag–0.7Cu alloy increased to 18.5 °C. It has been reported that [5] the large pasty range increases the tendency towards porosity and hot tearing due to the effect of alloy shrinkage and differential thermal contraction during solidification. A large pasty range may also causes manufacturing problems, such as increasing the sensitivity to vibration during wave soldering. In addition, the extensive pasty range may increase the probability of fillet lifting phenomena. For that reasons, the wide pasty range in the Sn–9Zn–1.5Ag–0.7Cu solder alloy is undesirable as far as the reflow process is concerned.

Table 3
Ultrasonic wave velocities (longitudinal V_l and shear V_s) and density (ρ) for the given solder alloys.

Alloy	V_l (m/s)	V_s (m/s)	ρ (kg/m^3)
Sn–9Zn	3375 ± 4	1831 ± 11	7290 ± 5
Sn–9Zn–1.5Ag	3339 ± 4	1803 ± 11	7238 ± 5
Sn–9Zn–0.7Cu	3366 ± 4	1827 ± 11	7354 ± 5
Sn–9Zn–1.5In	3372 ± 4	2002 ± 11	7265 ± 5
Sn–9Zn–1.5Ag–0.7Cu	3422 ± 4	2060 ± 11	7211 ± 5

The heat of fusion (ΔH) can be determined by the following generally accepted equation [20]:

$$\Delta H = \frac{kA}{m} \tag{10}$$

where k is a constant with the value of 2.64 for pure tin [19], which is defined as a calibration coefficient that depends on crucible shape, m is the mass of the sample, and A is the area under the endothermic peak. From Table 2, the values of ΔH obtained for different solders are 157.9, 21.6–88.5, 29.9–81.2, 127.4 and 45.9–56.1 J/g for the Sn–9Zn eutectic, Sn–9Zn–1.5Ag, Sn–9Zn–0.7Cu, Sn–9Zn–1.5In and Sn–9Zn–1.5Ag–0.7Cu alloys, respectively, showing that less energy is necessary to be consumed for melting the ternary and quaternary solder alloys. However, comparing these values with ΔH for some other solder alloys listed in Table 2. It is obvious that, the fusion heat of Sn–5Sb–3.5Ag is larger than that of the Sn–37Pb eutectic, whereas the present ternary and quaternary solder alloys exhibits the lowest one, which indicates that the Sn–9Zn–1.5Ag, Sn–9Zn–0.7Cu and Sn–9Zn–1.5Ag–0.7Cu alloys are considered as the most beneficial materials for saving energy.

3.3. Effect of alloy composition on the ultrasonic wave velocities and density

The numerically calculated values of the longitudinal-wave mode speed V_l and shear-wave mode speed V_s, propagating in the [1 0 0] and [1 1 1] directions, as well as the variation in densities ρ of the alloy compositions are listed in Table 3 and Fig. 3. It is seen that the separate additions of Ag, Cu and In elements decrease the V_l value of Sn–9Zn alloy from 3375 ± 4 to 3339 ± 4, 3366 ± 4 and 3372 ± 4 m/s, respectively, whereas the dual addition

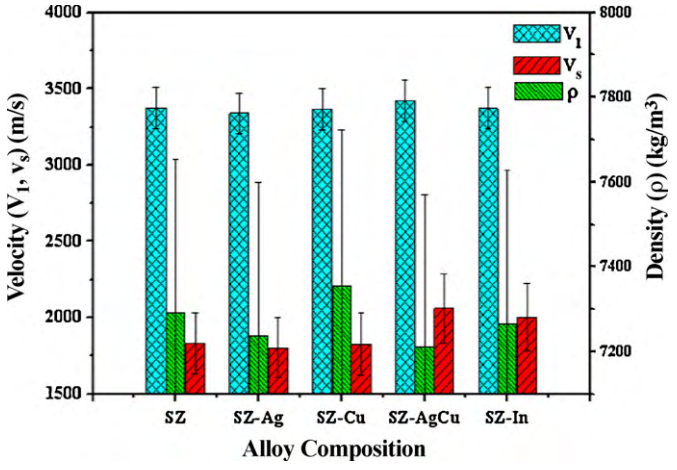

Fig. 3. Variation of ultrasonic wave velocities (longitudinal V_l and shear V_s) and density (ρ) with alloy composition.

of Ag and Cu increases it to 3422 ± 4 m/s. On the other hand, the V_s value of Sn–9Zn alloy decreases from 1831 ± 11 to 1803 ± 11 and 1827 ± 11 m/s with the addition of Ag and Cu, respectively, but it increases to 2002 ± 11 and 2060 ± 11 m/s with the In and dual addition of Ag and Cu, respectively. The first remarkable feature from these results is that the shear wave velocities is less than (about half of that of) longitudinal wave velocities. Thus the transit time of shear wave is more than (about double of) that of longitudinal wave velocity for the same thickness of the specimen. As the shear wave velocity is affected more than the longitudinal wave velocity due to any microstructural variation and the error in the measurement is also less, it can be concluded that ultrasonic shear wave velocity is a better parameter for microstructural characterization as compared to longitudinal wave velocity. The obtained results (Fig. 3 and Table 3) agree with the previous theoretical and experimental data [17], implying that our method for calculating the elastic properties is reasonable and reliable.

The second remarkable feature is that the rate of change of V_s is greater than that of V_l. Hence, using Eq. (8) in Section 2.4, the right hand side of Eq. (8) will be negative and Poisson's ratio υ value will vary opposite to V_l and V_s (or E and G) as seen in Table 3. Similar observations were obtained by Kumar et al. [17] who established that Poisson's ratio decreases with the increase in the elastic moduli and ultrasonic velocities for various solid isotropic materials. This result is easily understandable, as the only difference in alloy composition is the formation of IMCs due to the addition of In, Ag and Cu, all the other factors being the same. The physical meaning of change in ultrasonic wave velocities of solids is usually described in terms of the interaction of the ultrasonic wave front with the IMCs. The effect of IMCs on the ultrasonic wave velocity is attributable to variation in the stressed state of the material, which is determined by the difference between the volume extension coefficients as well as the elasticity moduli of the matrix and the densities of IMCs. Besides, the change in the volume fraction of proeutectic Sn and distribution of IMCs, which determine the condition of ultrasonic wave propagation and, in particular, affect the velocities of the longitudinal and transverse waves. In other words, the increase in wave velocities is most probably caused by the presence of more IMCs that acts as hard inclusions in a soft matrix. A similar dependence was found by Shalaby [7] as reported for Sn–9Zn lead-free solders with the addition of small amounts of In.

Table 3 shows also that all the densities ρ of the solders decrease with the addition of alloying elements except the Sn–9Zn–0.7Cu alloy, which showed significant increase in ρ value. However, the decrease or increase in ρ values may be due to the change in the axial ratio, densities and volume fraction of the newly developed IMCs in the ternary and quaternary solder alloys.

3.4. Effect of alloy composition on Poisson's ratio and elastic moduli

The Young's modulus E and Poisson's ratio υ are important for technological and engineering applications. The first one is defined as the ratio between stress and strain, and is used to provide a measure of the stiffness of the solid, i.e., the larger the value of E, the stiffer is the material. The second, the Poisson's ratio provides more information about the characteristics of the bonding forces than any of the other elastic constants. It has a value of between 0 and +0.5 depending on the compressibility of a material. So, the larger the υ is, the more ductile the alloy becomes [17,21]. It can be defined as the ratio of transverse strain (contraction) to axial strain (elongation) to be obtained in a uniaxial test. It is also quantify the material's resistance to dilatation and shearing [17]. Fig. 4 and Table 4 show that Poisson's ratio υ decreases with the addition of 1.5In or (1.5Ag + 0.7Cu). The results demonstrate that the Sn–9Zn, Sn–9Zn–1.5Ag and Sn–9Zn–0.7Cu alloys are much more ductile than the Sn–9Zn–1.5In and Sn–9Zn–1.5Ag–0.7Cu alloys. Since the value of υ for covalent materials is small (υ = 0.1), whereas for ionic materials a typical value of υ is 0.25 [22]. In our case the value of Poisson's ratio υ vary from 0.294 (Sn–9Zn–1.5Ag) to 0.216 (Sn–9Zn–1.5Ag–0.7Cu). This implies that a higher ionic contribution in inter-atomic bonding for these alloys should be assumed.

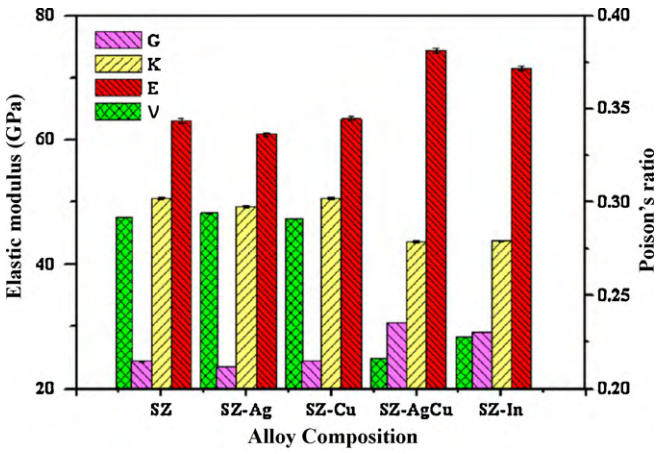

Fig. 4. Elastic modulus: shear modulus (G), bulk modulus (K), Young's modulus (E) and Poisson's ratio (υ) for Sn–9Zn (SZ), Sn–9Zn–1.5Ag (SZ–Ag), Sn–9Zn–0.7Cu (SZ–Cu), Sn–9Zn–1.5In (SZ–In) and Sn–9Zn–1.5Ag–0.7Cu (SZ–AgCu) alloys.

Since the first characteristic of a material that comes to mind is the stiffness. It is limited by the inter-atomic bonding energies and the connectivity, which are reflected macroscopically by elastic constants. Fig. 4 and Table 4 show also the variation of Young's modulus E for Sn–9Zn eutectic alloy with Ag, Cu and In contents. The E values for the as-cast alloys vary with chemical composition of IMCs and a minimum of about 60.9 ± 0.1 GPa is obtained for Sn–9Zn–1.5Ag alloy. The alloys containing In or dual addition of Cu and Ag generally have larger Young modulus (71.5–74.4 ± 0.1 GPa) than that of containing separate addition of Cu and Ag. It implies that the increase or decrease of the Young modulus with Sn–9Zn based alloys should be an intrinsic property of IMC phases owing to the characteristics of ionic bonding force of these compounds. In addition, the bulk modulus of Sn–9Zn–1.5Ag–0.7Cu (43.66 ± 0.3 GPa) is much smaller than that of the five solders alloys, and it implies that Sn–9Zn–1.5Ag–0.7Cu has high compressibility. However, according to our calculations in Table 4, the elastic constants decreased with increasing Poisson's ratio, and it was minimum when Poisson's ratio were maximum

Table 4
Experimental values of shear modulus (G), bulk modulus (K), Young's modulus (E), (G/K) ratio and Poisson's ratio (υ).

Alloy	G (GPa)	K (GPa)	E (GPa)	(G/K) ratio	υ
Sn–9Zn	24.43 ± 0.1	50.56 ± 0.3	63.1 ± 0.1	0.483	0.292 ± 0.008
Sn–9Zn–1.5Ag	23.52 ± 0.1	49.27 ± 0.3	60.9 ± 0.1	0.477	0.294 ± 0.008
Sn–9Zn–0.7Cu	24.55 ± 0.1	50.55 ± 0.3	63.4 ± 0.1	0.485	0.291 ± 0.008
Sn–9Zn–1.5In	29.11 ± 0.1	43.81 ± 0.3	71.5 ± 0.1	0.664	0.228 ± 0.008
Sn–9Zn–1.5Ag–0.7Cu	30.60 ± 0.1	43.66 ± 0.3	74.4 ± 0.1	0.700	0.216 ± 0.008

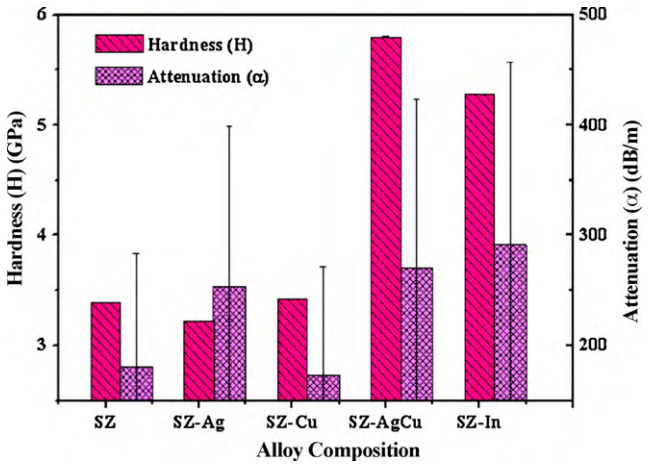

Fig. 5. Hardness (H) and attenuation coefficient (α) values for Sn–9Zn (SZ), Sn–9Zn–1.5Ag (SZ–Ag), Sn–9Zn–0.7Cu (SZ–Cu), Sn–9Zn–1.5In (SZ–In) and Sn–9Zn–1.5Ag–0.7Cu (SZ–AgCu) alloys.

and vice versa [17]. Similar observations were also obtained by Liu et al. [21].

A simple relationship, which empirically links the plastic properties of materials with their elastic moduli, was proposed by Pugh in [22]. The shear modulus G represents the resistance to plastic deformation, while the bulk modulus K represents their resistance to fracture [26]. The quotient of shear modulus to bulk modulus, G/K, can be considered as an indication of the extent of fracture range in metals as reported by Zhou et al. [23]. A low value and a high value of G/K are associated with ductility and brittleness, respectively. It has been assumed that the critical value which separates ductile and brittle materials is around 0.374–0.571; i.e., if G/K is less than 0.374–0.571, the material behaves in a ductile manner; otherwise the material behaves in a brittle manner [22,23]. In our case the low G/K ratios of 0.483, 0.447 and 0.485 for Sn–9Zn, Sn–9Zn–1.5Ag and Sn–9Zn–0.7Cu alloys, respectively, are associated with ductility, whereas a high values 0.664 and 0.700 correspond to the brittle nature of Sn–9Zn–1.5In and Sn–9Zn–1.5Ag–0.7Cu alloys, respectively (see Table 4). Although the above evaluation method is highly simplistic, it nevertheless indicates the tendency of ductility and brittleness for the five solder alloys.

3.5. Effect of alloy composition on the attenuation coefficient (α) and hardness (H)

Attenuation α is widely used as an ultrasonic parameter. It represents a relative energy loss experienced by an ultrasonic plane wave per unit length of a solid sample. Many authors believe that in polycrystalline materials attenuation is due mainly to scattering (reorientation and mode conversion of energy) by the grains and precipitates [8–11]. Scattering results in the interaction with the material defects comparable to one wavelength in size. For this reason, scattering depends on size, shape, type and volume fraction of the precipitates and the structure as well as chemistry of IMCs. Fig. 5 and Table 5 show that the value of α for Sn–9Zn specimen is 181 ± 57 dB/m. Additions of Ag and In to Sn–9Zn solder increase α value to 254 ± 57 and 291 ± 57 dB/m, respectively. In contrast, separate addition of Cu decreases α value to 173 ± 57 dB/m, whereas the dual addition of Ag and Cu increased it to 270 ± 57 dB/m. If we considered that the IMC is an oscillator with its own natural frequency of free oscillations, which appear under the action of the incident wave; as a result, the incident wave energy is reradiated by the oscillator. So, the scattered wave amplitude and frequency depend on the degree of damping of the oscillator by the surrounding medium and the natural oscillations of the oscillators. Hence, the variation in the value of α should not only be correlated with precipitation of the new IMC phases having different size, shape, and type as well as volume fraction, but also with the degree of homogeneity achieved by the matrix with the alloying element additions.

Table 5
Hardness (H) and attenuation coefficient (α) values for the given solder alloys.

Alloy	H (GPa)	α (dB/m)
Sn–9Zn	3.39 ± 0.07	181 ± 57
Sn–9Zn–1.5Ag	3.22 ± 0.07	254 ± 57
Sn–9Zn–0.7Cu	3.42 ± 0.07	173 ± 57
Sn–9Zn–1.5In	5.28 ± 0.07	291 ± 57
Sn–9Zn–1.5Ag–0.7Cu	5.80 ± 0.07	270 ± 57

However, a close correlation between the attenuation coefficient of the material and pasty range can be observed in the present work. Due to the fact that the large pasty range increases the sensitivity to vibration during wave soldering, the attenuation is taken into account during wave soldering. In this case, it is possible to explain the increase in α value with increasing the pasty range by increasing the sensitivity to vibration during wave soldering. The highest values of α in the Sn–9Zn–1.5In, Sn–9Zn–1.5Ag and Sn–9Zn–1.5 Ag–0.7Cu solders compared to the other solders implies that their resonant life were shorter than that of the other solders. The shorter vibration life can be ascribed to localize intergranular cracking linked by their IMCs, which promotes the vibration crack propagation mechanism. This argument might provide useful guideline for the development of lead-free solders by appropriate choice of components with α control strategy. However, more studies are needed to establish this argument.

Fig. 5 and Table 5 show that the hardness value of Sn–9Zn is 3.39 ± 0.07 GPa. The H values of Sn–9Zn–1.5In and Sn–9Zn–1.5Ag–0.7Cu alloys increased up to 5.28 ± 0.07 and 5.80 ± 0.07 GPa, respectively. In contrast, slightly change in the H values has been observed in Sn–9Zn–1.5Ag and Sn–9Zn–0.7Cu alloys. The H values for the two alloys are 3.42 ± 0.07 and 3.22 ± 0.07 GPa, respectively. However, it is possible to explain the increase in hardness not only by the increase in the volume fraction of IMCs but also with the nature of the atomic bonding forces between the constituents of IMCs, which are reflected macroscopically by the other elastic constants. In other words, the change in hardness results in increasing the initial status of IMCs precipitates of the material and its structural evolution, which reflects as an increase of the effective acting stress at continuum scale due to the inelastic volume conservation, as well as strain localization and geometry changes. For that reasons, the increase in the hardness value is attributable to the presence of hard IMCs, which acts as hard inclusions in the soft matrix.

3.6. Tensile properties

A stress–strain approach was employed to evaluate the mechanical properties for the five alloys in this study. Figs. 6 and 7 show the typical tensile stress–strain curves of the lead-free solder specimens at a constant strain rate of 1.8×10^{-3} s^{-1} and $T = 25$ °C. The average values of ultimate tensile strength UTS, yield stress σ_y, Young modulus E and ductility are given in Table 6. The UTS values of the as-solidified Sn–9Zn eutectic, Sn–9Zn–1.5Ag, Sn–9Zn–0.7Cu, Sn–9Zn–1.5In and Sn–9Zn–1.5Ag–0.7Cu alloys were 41.9, 56.3, 45.2, 53.3 and 49.4 MPa, respectively. The elongations to failure for the Sn–9Zn eutectic, Sn–9Zn–1.5Ag, Sn–9Zn–0.7Cu, Sn–9Zn–1.5In and Sn–9Zn–1.5Ag–0.7Cu alloys were 21.3, 33.8, 21.7, 22.3 and 23.3%, respectively. The Sn–9Zn–1.5Ag alloy had both the highest UTS and elongation. Additionally, the increase in its ductility is

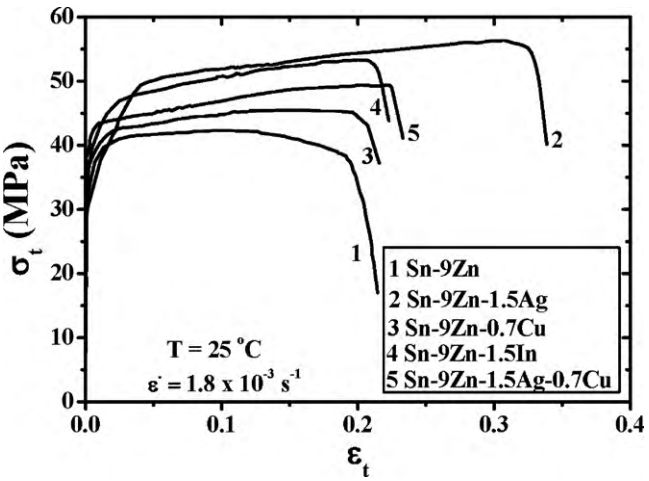

Fig. 6. Comparative tensile stress–strain curves obtained at $T = 25\,^{\circ}C$ and $\dot{\varepsilon} = 1.8 \times 10^{-3}\,s^{-1}$ for (1) Sn–9Zn, (2) Sn–9Zn–1.5Ag, (3) Sn–9Zn–0.7Cu, (4) Sn–9Zn–1.5In and (5) Sn–9Zn–1.5Ag–0.7Cu alloys.

accomplished without sacrificing their mechanical strength. However, the separate addition of Cu and In or the dual addition of Ag and Cu had no significant contribution to the elongation but had a positive effect on the mechanical strength of the Sn–9Zn samples. On the other hand, strain hardening instead of strain softening occurred in both as-solidified ternary and quaternary alloys, which improves the UTS and yield stress σ_y in these alloys. Conversely,

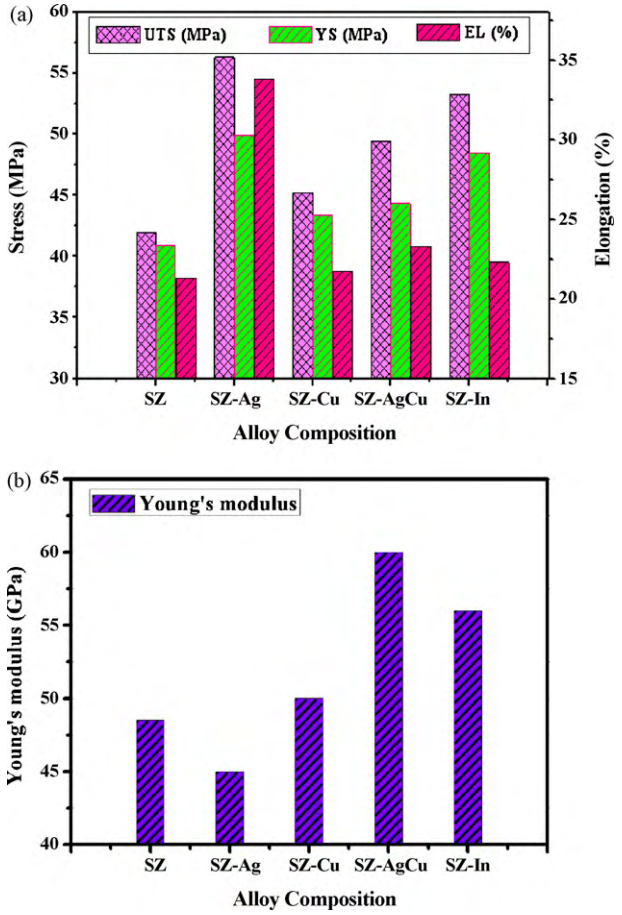

Fig. 7. Mechanical properties of the samples: (a) tensile strength and elongation (UTS: ultimate tensile strength; YS: yield strength; EL: total elongation) and (b) Young's modulus.

Table 6
Tensile properties of the solders Sn–9Zn, Sn–9Zn–1.5Ag, Sn–9Zn–0.7Cu, Sn–Zn–1.5In and Sn–9Zn–1.5Ag–0.7Cu solder alloys at $T = 25\,^{\circ}C$ and $\dot{\varepsilon} = 1.8 \times 10^{-3}\,s^{-1}$.

Alloy	UTS (MPa)	(σ_y) (MPa)	Elongation (%)	E (GPa)
Sn–9Zn	41.9	40.9	21.3	48.5
Sn–9Zn–1.5Ag	56.3	49.9	33.8	45.0
Sn–9Zn–0.7Cu	45.2	43.4	21.7	50.0
Sn–9Zn–1.5In	53.3	48.5	22.3	56.0
Sn–9Zn–1.5Ag–0.7Cu	49.4	44.3	23.3	60.0

the absence of work hardening exhibited by Sn–9Zn solder also leads to reduce their mechanical strength. In Sn–9Zn alloy, dynamic recovery also was considered to contribute to the absence of strain hardening. As a result, it has been suggested that the plastic deformation was mostly carried by the simultaneous deformation of the IMCs particles and matrix, which results in some strengthening mechanism occurred in the ternary and quaternary solder alloys. These results are consistent with the findings of other researchers working on Sn–9Zn based solders [24].

The values of Young's modulus E obtained from the slope of the stress–strain curves are listed in Table 6 and Fig. 7b. In engineering practice, these E values are described as the static modulus, which is generally referred as the apparent or effective elastic modulus since the behavior is obviously not purely elastic. The comparison of static modulus values with dynamic modulus measured by the ultrasonic wave method (see Table 4), one shows a slight discrepancy between both techniques. It can be noted that the values of Young's modulus obtained using novel ultrasonic technique is larger than that found using the tensile stress–strain method. This may be regarded as an overestimation in real cases. Nevertheless, it remains acceptable if one considers the fact that the elastic modulus obtained from the slope of the stress–strain curve usually includes small inelastic deformations or time-dependent deformations such as creep. As a result, the apparent static elastic modulus is usually smaller than the dynamic modulus measured by the acoustic or ultrasonic wave method, which largely eliminates the inelastic deformation due to rapid wave propagation. A similar trend has been reported by [25,26], which showing the obvious effects of inelastic deformations on the elastic modulus.

4. Conclusions

In summary, we have investigated the structural, elastic and thermal properties of Sn–Zn based solders containing small amount of Ag, In and Cu elements. We calculated the sound velocities and densities for the investigated alloys. We derived the hardness, the attenuation coefficient, the bulk and shear moduli, Young's and Poisson's ratio for Sn–9Zn eutectic, Sn–9Zn–0.7Cu, Sn–9Zn–1.5Ag, Sn–9Zn–1.5In and Sn–9Zn–1.5Ag–0.7Cu solders. The results are summarized as follows:

1. From microstructure examination, some new phases are developed compared to Sn–9Zn eutectic solder alloy such as AgZn, γ-Ag_5Zn_8 and ε-$AgZn_3$ for Ag-containing solder, Cu_6Sn_5, γ-Cu_5Zn_8 and ε-$CuZn_5$ for Cu-containing solder, and In_3Sn for In-containing solder, along with the peaks of β-Sn phase and α-Zn phase in all alloys.
2. Alloying of Cu, In and Ag resulted in reducing the heat of fusion and solidus temperature besides broadening the pasty range.
3. The Sn–9Zn–1.5Ag lead-free solder proved to be promising in that it gave good combination of higher UTS and elongation than the other three alloys, which was possible due to the formation of hard and soft Ag–Zn, γ-Ag_5Zn_8, ε-$AgZn_3$ precipitates.
4. Both the hardness and reduced modulus increase as the Poisson's ratio of the alloy decreases. The elastic proper-

ties can be correlated with the formation of the new IMC phases.

5. By analyzing the quotient of shear modulus to bulk modulus, it was found that the Sn–9Zn, Sn–9Zn–1.5Ag and Sn–9Zn–0.7Cu alloys are ductile solders whereas, the Sn–9Zn–1.5In and Sn–9Zn–1.5Ag–0.7Cu alloys are brittle in nature.
6. The value of Poisson's ratio υ varies from 0.294 (Sn–9Zn–1.5Ag) to 0.216 (Sn–9Zn–1.5Ag–0.7Cu). This implies that a higher ionic contribution in interatomic bonding for these alloys should be assumed.
7. The solving for most manufacturing problems may be occur by appropriate choice of components with α and υ control strategy.

References

[1] J. Shen, Y.C. Chan, J. Alloys Compd. 477 (2009) 552–559.
[2] W.K. Liou, Y.W. Yen, K.D. Chen, J. Alloys Compd. 479 (2009) 225–229.
[3] X. Wei, H. Huang, L. Zhou, M. Zhang, X. Liu, Mater. Lett. 61 (2007) 655–658.
[4] S.H. Wang, T.S. Chin, C.F. Yang, S.W. Chen, C.T. Chuang, J. Alloys Compd. 497 (2010) 428–431.
[5] A.A. El-Daly, Y. Swilem, M.H. Makled, M.G. El-Shaarawy, A.M. Abdraboh, J. Alloys Compd. 484 (2009) 134–142.
[6] A.A. El-Daly, A.E. Hammad, Mater. Sci. Eng. A (2010), doi:10.1016/j.msea.2010.04.078.
[7] R.M. Shalaby, Cryst. Res. Technol. (2010), doi:10.1002/crat.201000022.
[8] S. Ganeshan, S.L. Shang, Y. Wang, Z.K. Liu, J. Alloys Compd. 498 (2010) 191–198.
[9] J.X. Yi, P. Chen, D.L. Li, X.B. Xiao, W.B. Zhang, B.Y. Tang, Solid State Commun. 150 (2010) 49–53.
[10] S.M. Foiles, Scripta Mater. 62 (2010) 231–234.
[11] H.C. Hsu, S.K. Hsu, S.C. Wu, C.J. Lee, W.F. Ho, Mater. Charact. (2010), doi:10.1016/j.matchar.2010.05.003.
[12] A. Hamidani, B. Bennecer, B. Boutarfa, Mater. Chem. Phys. 114 (2009) 732–735.
[13] M.S. Gaafar, Y.B. Saddeek, L. Abd El-Latif, J. Phys. Chem. Solids 70 (2009) 173–179.
[14] Y.B. Saddeek, M.S. Gaafar, S.A. Bashier, J. Non-Cryst. Solids 356 (2010) 1089–1095.
[15] M.S. Gaafara, N.S. Abd El-Aal, O.W. Gerges, G. El-Amir, J. Alloys Compd. 475 (2009) 535–542.
[16] M.S. Gaafar, Y.B. Saddeek, L. AbdEl-Latif, J. Phys. Chem. Solids 70 (2009) 173–179.
[17] A. Kumar, T. Jayakumar, B. Raj, K.K. Ray, Acta Mater. 51 (2003) 2417–2426.
[18] J.E. Lee, K.S. Kim, M. Inoue, J. Jiang, K. Suganuma, J. Alloys Compd. 454 (2008) 310–320.
[19] A.A. El-Daly, Y. Swilem, A.E. Hammad, J. Alloys Compd. 471 (2009) 98–104.
[20] A.A. El-Daly, Y. Swilem, A.E. Hammad, J. Mater. Sci. Technol. 24 (6) (2008) 921–925.
[21] Y.H. Liu, G. Wang, D.Q. Zhao, M.X. Pan, W.H. Wang, Science 315 (2007) 1385.
[22] M. Hichour, D. Rached, M. Rabah, S. Benalia, R. Khenata, F. Semari, Physica B 404 (2009) 4034–4038.
[23] W. Zhou, L. Liu, B. Li, P. Wua, Q. Song, Comput. Mater. Sci. 46 (2009) 921–931.
[24] S.K. Das, A. Sharif, Y.C. Chan, N.B. Wong, W.K.C. Yung, J. Alloys Compd. 481 (2009) 167–172.
[25] S. Wiese, A. Schubert, H. Walter, R. Dudek, F. Feustel, E. Meusel, B. Michel, Proceeding of the 51st Electronic Components and Technology Conference, 2001, pp. 890–902.
[26] F.Y. Hung, T.S. Lui, L.H. Chen, N.T. He, J. Alloys Compd. 457 (2008) 171–176.